

Influence of channelling on heating in ice-sheet flows

Richard C. A. Hindmarsh

British Antarctic Survey, Cambridge, GREAT BRITAIN

Abstract. Ice-sheet flows can be channelled by perturbations in the basal topography or in the sliding coefficient. These lead to spatial variation in the steady profile, the flux and the dissipative heating. This paper examines the linearized theory of heating variations, showing that the map plane aspect ratio of the basal perturbation has a dominating effect on the qualitative behaviour. For ribbing transverse to the direction of flow, maximum heating occurs over bedrock and sliding viscosity highs. When flow-parallel channelling occurs maximum heating occurs over bedrock lows and sliding viscosity lows. These results are used to examine symmetry-breaking behaviour of numerical thermoviscous ice-sheet models in terms of a dissipation-driven creep instability.

Introduction

Whether and why ice-sheets exhibit symmetry-breaking transitions into faster streaming flows is a central issue of modern glaciology. (Here, symmetry breaking means the existence of periodicities in the solution which are not present in the governing equations or boundary conditions). Recent work on thermally-coupled ice sheet flow has emphasized the importance of flow channelling on the spatial distribution of dissipative heating *Payne & Dongelmans* [1997]; *Payne & others* [2000]. This channelling can be due to (i) basal topography and (ii) variations in the ice viscosity or sliding viscosity. In particular, these authors suggest that a feedback between heating, temperature and viscosity may cause unstable or symmetry-breaking behaviour.

Such thermoviscous instabilities are related to the notion of a 'creep instability' [*Clarke & others*, 1977], where increased temperatures lead to increased deformation rates and increased heating. There exist a further set of instability mechanisms by which perturbations to the flow that arise from ice or sliding viscosity variations affect the surface topography, stress and flow fields and through these the spatial distribution of dissipative heating. An additional feedback loop is thereby closed because spatial variations in viscosity, which forces the heating, can be caused by temperature variations.

Plausibility reasoning using these feedback concepts has been used to support the validity of results of numerical computations of symmetry breaking in ice-sheet flows [*Payne & others*, 2000]. Some mathematical analyses which inform about how channelling affects heating distributions and which are pertinent to these arguments are presented in this paper. Flow down an infinite plane with a flat bed and uniform sliding coefficient provides a base case, and a linearized

model capable of dealing with perturbations in the basal properties (topography or sliding viscosity) is derived. This is used to compute the perturbed ice surface topography under shallow ice approximation (SIA). This flow is known to be stable [*Nye*, 1959].

Total dissipation integrated over the thickness of ice as a function of horizontal position is proportional to the scalar product of the flux and ice surface slope under the SIA [*Hindmarsh*, 1990]. The surface perturbation provides enough information to compute the perturbed column averaged heating dissipation. In shearing flows respecting the shallow ice approximation the dissipation occurs near the base, and when sliding is occurring the heating happens right at the base. Since the rate factors controlling both processes are strongly temperature dependent, a fairly direct link between dissipation and deformation is anticipated.

A significant extension of the SIA has been presented in models of ice streams where significant amounts of energy are dissipated in vertical sections at the lateral margins of highly-lubricated ice streams [*Echelmeyer & others*, 1994; *Harrison & others*, 1998; *Jacobson & Raymond*, 1998; *Raymond*, 2000] rather than at the base as in the present analysis, but represents a developmental end-member case since for this situation to arise, significant amounts of dissipation must have occurred at the base in order to lubricate it so that drag transfers to the lateral margins.

Adjustment of the ice surface changes both thickness and slope, which affects the flux. Ice surface highs do not necessarily correspond to bedrock highs [*Budd*, 1970; *Hutter*, 1983], implying that phasing of dissipation with variations in bed properties is not simple. Here we explore this phasing, and shows that the phasing depends strongly on the map plane aspect ratio of forcing by for example bed topography or sliding viscosity. The results illuminate the extent to which observations of symmetry-breaking behaviour in numerical ice-sheet models can be explained in terms of a dissipation-driven thermoviscous instability.

Linearized model

We consider flow down an infinitely long and broad plane, with coordinates (x, y, z) and gravity components given by $g(\varepsilon, 0, -1)$. We represent the horizontal coordinates (x, y) by the vector \mathbf{r} . We are assuming ε^2 to be small; however, ε is not a perturbation parameter in the linearization below. Wavelengths of undulations which give rise to surface effects are much larger than the ice thickness in this analysis and the mechanics can thus be described by the shallow-ice approximation [*Hutter*, 1983]. Thus the analysis does not apply to very well-lubricated streams where most of the drag is at the flanks.

Flow of ice occurs either by (i) internal deformation according to the viscous relationship $\mathbf{e} = A_c |\dot{\gamma}|^{n-1} \dot{\gamma}$ [*Paterson*, 1994] where \mathbf{e} is the deformation rate tensor, $\dot{\gamma}$ is a second

Copyright 2001 by the American Geophysical Union.

Paper number 2000GL012666.
0094-8276/01/2000GL012666\$05.00

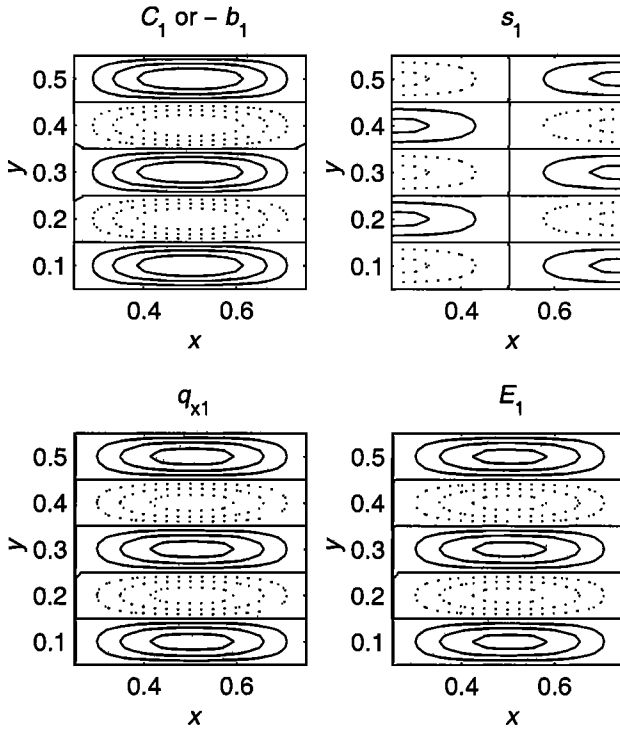


Figure 1. Contours of forcing function (the sliding coefficient) C_1 and computed surface response s_1 , downstream flux q_{x1} and dissipative heating E_1 for channelled forcing. Heating is concentrated over areas where sliding (C_1) is greater or the bedrock is lower.

invariant of the deviator stress tensor τ , and A_c is a rate factor or (ii) by sliding described by a relation of the form $\mathbf{u}_b = A_s |\mathbf{T}|^{\ell-1} \mathbf{T}$, where \mathbf{u}_b is the sliding velocity and \mathbf{T} is the basal tangential traction vector. For simplicity we consider flow by one or other of these mechanism; the results of the analysis are expected to generalise to combinations of these two mechanisms.

The surface, base and thickness of the ice are denoted by $s(x, y, t)$, $b(x, y, t)$ and $H(x, y, t)$ respectively. We define the quantities ν, m and C as follows. For internal deformation $\nu = n, m = n + 2, C = \frac{2}{n+2} A_c (\rho g)^\nu$, while for sliding $\nu = \ell, m = \ell + 1, C = A_s (\rho g)^\ell$ where ρ_s is the density of ice and g is the acceleration due to gravity.

We expand $s = s_0 + s_1$ etc., where $s_1 \ll s_0$. At zeroth-order, we set H_0 constant, $b_0 = 0, s_0 = H_0$ and define the zeroth order flux $Q_0 = C_0 (\rho g)^\nu H_0^m \varepsilon^\nu$. The first-order flux vector \mathbf{q}_1 is [Hindmarsh, 2000]

$$\mathbf{q}_1 = Q_0 \left[\frac{m s_1 - b_1}{H_0} - \nu \frac{\partial_x s_1}{\varepsilon} + \frac{C_1}{C_0}, \quad -\frac{\partial_y s_1}{\varepsilon} \right], \quad (1)$$

This expresses the perturbed flux in terms of the perturbed surface profile, viscosity and bed profile. We construct bed property perturbations in terms of a wavenumber vector \mathbf{k} , which under will also be the wavelength of the surface topography. Defining $\mathbf{r} = (x, y)$ we write $b_1 = \hat{b}_1 \exp(-i\mathbf{k} \cdot \mathbf{r})$ etc., where hatted quantities denote the Fourier Transform and $i^2 = -1$. Taking the Fourier transform of the first-order continuity equation and prescribing steady state leads to an expression for the steady surface

elevation [Hindmarsh, 2000]

$$\hat{s}_1 = \frac{i\varepsilon k_x}{(i\varepsilon k_x \frac{m}{H_0} - \nu k_x^2 - k_y^2)} \left(\frac{m}{H_0} \hat{b}_1 - \frac{\hat{C}_1}{C_0} \right). \quad (2)$$

The heating distributions are $E_0 = Q_0 \rho g \varepsilon$, $E_1 = \rho g (q_{1x} \varepsilon - q_{0x} \partial_x s_1)$. Then, using the first-order flux (1) and (2) to eliminate \hat{s}_1 we obtain

$$\frac{\hat{E}_1}{E_0} = \frac{(k_x^2 - k_y^2)}{(\varepsilon i k_x \frac{m}{H_0} - \nu k_x^2 - k_y^2)} \left(\frac{\hat{C}_1}{C_0} - \frac{m \hat{b}_1}{H_0} \right), \quad (3)$$

$$\hat{E}_1 = i E_0 (k_x^2 - k_y^2) \hat{s}_1 / \varepsilon k_x. \quad (4)$$

Applications

We can immediately deduce from relationships (2), (3) and (4) that: (i) When wave-numbers are equal, there is no heating perturbation; (ii) Where $k_x > (<) k_y$ the phasing of heating with steady surface elevation for both bedrock and sliding coefficient perturbations is $+(-)\pi/2$. (iii) Phasing of heating with forcing differs by π depending on whether the x - or y -wavelengths are the greater. (iv) There is a dependence of phasing on absolute wavelength as well as map-plane wavelength ratio.

Scaling reduces the number of parameters. We set the thickness scale equal to H_0 , and choose the length scale $[X] = [H]/\varepsilon$. This corresponds to the unit length in the dimensionless system. Similarly we set the rate factor and heating scales to C_0, E_0 . In dimensionless form (2) and (3) are

$$\hat{s}_1 = i k_x (m \hat{b}_1 - \hat{C}_1) / D, \quad (5)$$

$$\hat{E}_1 = (k_x^2 - k_y^2) (\hat{C}_1 - m \hat{b}_1) / D. \quad (6)$$

where $D \equiv (i m k_x - \nu k_x^2 - k_y^2)$. The length scale, and in particular the physical wavelength corresponding to unit wavelength in the dimensionless system, depend strongly on the thickness and the slope. The smaller the slope, the larger this wavelength. Typically $[H] = (1 \rightarrow 3)$ km, $\varepsilon = (10^{-3} \rightarrow 10^{-2})$, implying $[X] = (100 \rightarrow 3000)$ km. Since a typical ice stream is around 500 km in length, and the shallow ice approximation (for moderately lubricated ice streams) becomes invalid for wavelengths comparable with the ice thickness (< 10 km), we investigate the behaviour of the solution in the range of dimensionless wavelengths $(0.002 \rightarrow 5)$. However, near the margin of a land-based ice-sheet, slopes becomes greater and thickness less, meaning that $[X] \ll 100$ km and that features of interest can have dimensionless wavelength $\gg 1$. In consequence we consider the range of dimensionless wavelengths $\lambda = (0.002 \rightarrow 100)$, understanding that values greater than 5 may only be representative near the margin of land-based ice-sheets.

Figures 1 and 2 present computations of surfaces of s_1, q_{x1} and E_1 for $[\lambda_x, \lambda_y] = [1, 0.2]$ and $[0.2, 1]$ respectively. The two cases correspond to channelled and ribbed flows. In this study, $\nu = 3$ and $m = 4$. The forcing functions are created by the superposition of two washboards, i.e. $b_1 = \hat{b}_1 \{\exp(-i\mathbf{k}_+ \cdot \mathbf{r}) + \exp(-i\mathbf{k}_- \cdot \mathbf{r})\}$ etc., where $\mathbf{k}_+ = 2\pi(1/\lambda_x, 1/\lambda_y)$, $\mathbf{k}_- = 2\pi(1/\lambda_x, -1/\lambda_y)$. The figures are qualitative indicators of the response, and show the phasing of solution fields. Solid lines represent positive perturbations, while dotted lines show negative perturbations. The choice of the forcing functions (b_1 and C_1)

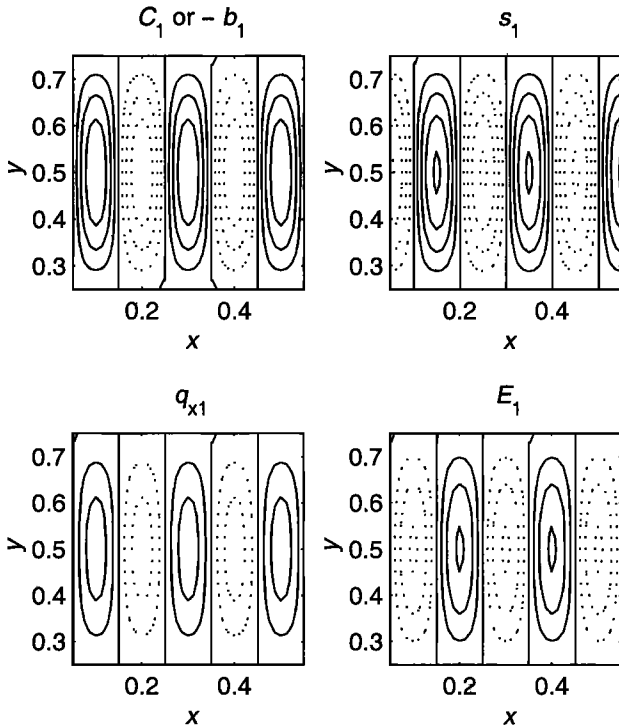


Figure 2. Same as Figure 1 for *ribbed* forcing. Heating is concentrated over areas where sliding (C_1) is decreased or the bedrock is elevated.

divide the domain into a checkerboard of positive and negative subdomains, inducing a checkerboard pattern in the response functions s_1, q_{x1}, E_1 , which can be offset in the x -direction with respect to the forcing. Within each of these subdomains, forcing and response function are monotone; all contours have increasing or decreasing values.

For the parameter values selected, where the flow is channelled, dissipation is in phase with increased slipperiness and bedrock troughs, while for flows obstructed by transverse ribbing, dissipation is in phase with decreased slipperiness and bedrock highs. For both channelled and ribbed forcing the surface elevation is $\pm\pi/2$ out of phase with viscosity and topography respectively.

The general applicability of these observations can be deduced by inspecting equations (5), (6). These show that for $k_x \gg 1$ the denominator is real, leading to the $\pi/2$ phase difference for the surface and the $\pm\pi$ phasing for the heating. If $k_x, k_y \ll 1$, the denominator is imaginary, and the heating phasing is $\pm\pi/2$ relative to the basal perturbation. For reasons outlined above, this is only likely to happen near the thin margins of land-based ice-sheets.

A case where variations in basal properties occur along the axes of channels is shown in Figure 3. Here $b_1 = \hat{b}_1 \{ \exp(-ik_x x) + \exp(-ik_y y) \}$, with $[\lambda_x, \lambda_y] = [0.50, 2]$. The surface topography shows no channelling, but there is channelling of flux. The heating occurs where the flow is channelled, but is accentuated in shallower areas or more viscous areas, as with the ribbed flow example above.

Figure 4 presents surfaces of $|\hat{E}_1|$ and $|\hat{s}_1|$ and the corresponding phase angles plotted against the two wavenumber components. The heating shows an obvious dependence on the aspect ratio, and a very weak dependence on the abso-

lute wavelength, except in the very long wavelength regime. For unit aspect ratio, one has a surface response which induces absolutely no heating response.

Concluding Discussion

Dissipation-driven thermoviscous instabilities are held to be responsible for much ice stream variability [Payne & Don-gelmans, 1997; Payne & others, 2000], and differences may exist in the characteristics of thermoviscous instabilities for plane flow (where no channelling can occur), 2D ribbed or channelled flows in areas where wavelengths either less than the critical wavelength H/ϵ , or areas close to the margin of a land-based ice-sheet where features with wavelength greater than H/ϵ can exist. For example, where the sliding viscosity exhibits flow-transverse ribbing, maximum heating occurs where the viscosity is greatest and the ice is cooler. If this warming were unstable and the ice became warmer than the mean value, dissipation would decrease to less than the mean value and the warming would cease. In consequence, this ribbed configuration cannot lead to a steady broken symmetry unless horizontal advection significantly affects phasing relationships. However, a warming instability could excite transient behaviour (e.g. oscillations).

In contrast, for channelled flow, the opposing phasing means warming will occur in areas of depressed viscosity (corresponding to warmer ice). An unstable warming would depress the sliding viscosity even further, stabilizing steady patterns. (This could lead eventually lead to the formation of ice streams where the lubrication was so high that dissipation occurred mainly at the margins.) It does not directly suggest a mechanism whereby streams form and then oscillate. This is significant because of the many observations of variability in channelled flows [Alley & Bind-schadler, 2001].

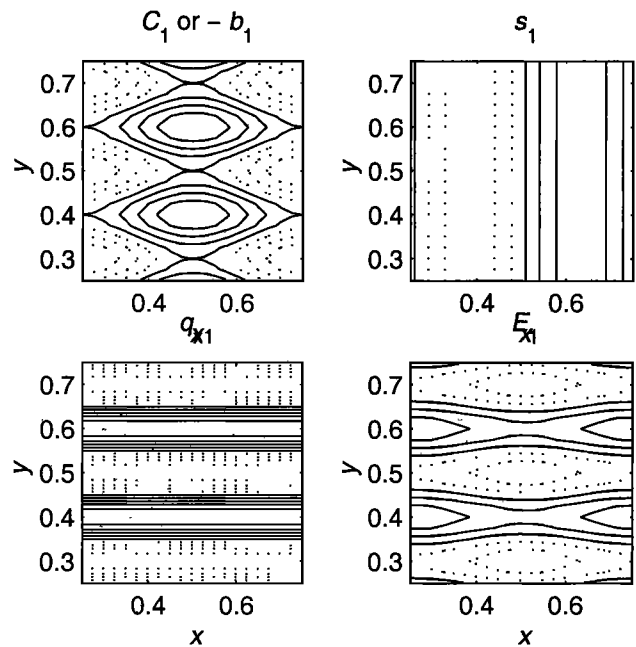


Figure 3. Same as Figure 1 for channels with axial variation. Heating is higher in channels but within these channels is concentrated over areas where sliding (C_1) is decreased or the bedrock is elevated.

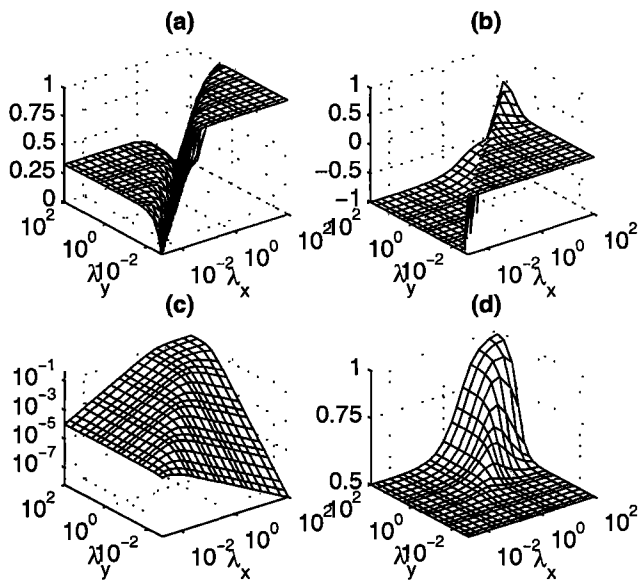


Figure 4. (a) Surface of $|\hat{E}_1|$ against wavelengths λ_x, λ_y . (b) Surface of phase relationships of the heating (normalised by π) against wavelengths λ_x, λ_y . Points where the two wavelengths are equal induce a zero response in the heating, meaning that the phasing is not defined. (c) Surface of $|\hat{s}_1|$ against wavelengths λ_x, λ_y . (d) Surface of phase relationships of the surface (normalised by π) against wavelengths λ_x, λ_y .

Reports of numerical calculations indicate that for plane flow, symmetry-breaking instabilities leading to oscillations do occur Payne [1995]; Greve & MacAyeal [1996]; Pattyn [1996]. Plane flow computations have never shown steady pattern formation in basal temperatures. These observations accord with the qualitative discussion above; if the system breaks symmetry in plane flow, it cannot be into a steady state.

In two-dimensional flow, symmetry-breaking leading to channel formation has also been observed. The resulting patterns comprise both steady features [Payne & Dongelmans, 1997; Payne & others, 2000], some where the ice is thin Payne & Baldwin [1999], and also oscillatory, possibly chaotic, features Payne & Dongelmans [1997]; Payne [1998]. The discussion above suggests that symmetry breaking of channelled flows is more likely to lead to steady features. However, longitudinal variations within channels could be unstable in the manner described above for ribbed obstructions because they induce the unstable pattern of dissipation. The difference between this case and the channelled case is quite subtle and it is not clear whether it accounts for the difference between computed transient and steady channelled flows in ice-sheet models.

Heating, surface topography and basal forcing relationships are not straightforward, and one should be wary

of using plausibility reasoning to justify the results of numerical calculations. More theory is needed to understand symmetry breaking in natural and modelled ice flows.

References

- Alley, R.B. and R.A. Bindschadler, *The West Antarctic Ice Sheet Behavior and Environment*, Antarctic Research Series 77, AGU, Washington, 2001.
- Budd, W.F. Ice flow over bedrock perturbations, (1970), *J. Glaciol.*, 9(), 19-27, 1970.
- Clarke, G.K.C., U. Nitsan and W.S.B. Paterson. Strain heating and creep instability in glacier and ice sheets, *Rev. Geophys. and Space Physics*, 15(2), 235-47, 1977.
- Echelmeyer K.A., W.D. Harrison, C. Larsen and J.E. Mitchell, The role of the margins in the dynamics of an active ice stream. *J. Glaciol.*, 40(136), 527-538, 1994
- Greve, R. and D.R. MacAyeal, Dynamic/thermodynamic simulations of Laurentide ice sheet instability. *Ann Glaciol.* 23, 328-335, 1996.
- Harrison WD, K.A. Echelmeyer and C.F. Larsen, Measurement of temperature within a margin of Ice Stream B: implications for margin migration and lateral drag, *J. Glaciol.*, 44(), 615-624, 1998
- Hindmarsh, R.C.A., Time-scales and degrees of freedom in the evolution of continental ice-sheets, *Trans. Roy. Soc. Ed. Earth Sci.* 81 371-84, 1990.
- Hindmarsh, R.C.A. Sliding over anisotropic beds, *Ann. Glaciol.*, 30, 137-154, 2000.
- Hutter, K., *Theoretical Glaciology*, Reidel, 1983.
- Jacobson, P.H. and C.F. Raymond, Thermal effects on the location of ice stream margins. *J. Geophys. Res.*, 103(B6), 12111-12122, 1998.
- Nye, J.F. The motion of ice sheets and glaciers, *J. Glaciol.*, 3, 493-507, 1959.
- Paterson, W.S.B. *The Physics of Glaciers*, Pergamon, 1994.
- Pattyn, F. Numerical modelling of a fast flowing outlet glacier: experiments with different basal conditions, *Ann. Glaciol.*, 23, 237-246, 1996.
- Payne, A.J. Limit cycles in the thermal regime of ice sheets, *J. Geophys. Res.*, 100(B3), 4249-63, 1995.
- Payne, A.J. Dynamics of the Siple Coast ice streams, West Antarctica: results from a thermomechanical ice sheet model, *Geophys. Res. Lett.*, 25(16), 3173-3176, 1998
- Payne, A.J. and P. Dongelmans, Self-organization in the thermomechanical flow of ice-sheets, *J. Geophys. Res.*, 102(B6), 12219-12233, 1997.
- Payne A.J. and D.J. Baldwin, Thermo-mechanical modelling of the Scandinavian ice sheet: implications for ice-stream formation. *Ann. Glaciol.*, 28, 83-89, 1999.
- Payne A.J. and ten others, Results from the EISMINT intercomparison: the effects of thermo-mechanical coupling. *J. Glaciol.*, 46(153), 227-238, 2000.
- Raymond, C.F., Energy balance of ice streams. *J. Glaciol.*, 46(155), 665-674, 2000

Richard C.A. Hindmarsh, British Antarctic Survey, Natural Environment Research Council, High Cross, Madingley Road, Cambridge CB3 0ET, GREAT BRITAIN.

(Received November 21, 2000; revised July 29, 2001; accepted August 1, 2001.)